Challenge Journal of Structural Mechanics

Research Article

Boundary plate influence on tie bars axial force demands in composite plate shear walls–concrete filled

Erkan Polat [a,*]

[a] *Department of Civil Engineering, Munzur University, 62000 Tunceli, Türkiye*

ABSTRACT

In composite plate shear walls–concrete filled (C-PSW/CF), there is an indeterminate flow of force between concrete, steel plate and tie bars. Finite element methods (FEM) are frequently used to verify this force flow. The theoretical models available in the literature to predict the tie bar maximum axial force demands were based on walls without boundary plates. The finding in this study is intended to help understand whether current theoretical approaches are conservative and can be applied to boundary plate walls as well. Within the scope of this study, tie bar axial force demands for walls with boundary plates consisting of planar and round shapes and without boundary plates were investigated and compared. For this, a previously benchmarked finite element (FE) wall model was considered and configured to have no boundary plate and have planar and round boundary plates. FE models were analyzed under monotonic lateral displacement up to 4% drift ratio. Passive lateral pressures and transverse force variations on the planar and round boundary plates were investigated.

ARTICLE INFO

Article history:
Received 1 June 2022
Revised 25 August 2022
Accepted 23 September 2022

Keywords:
Composite plate shear walls
Concrete-filled
Tie bar
Boundary
Axial force

1. Introduction

In composite plate shear walls – concrete filled (C-PSW/CF) there is an indeterminate flow of forces between the wall parts (i.e., steel plates, infill concrete and tie bars). This force flow provides composite behavior and achieved by axial and shear force transfer between the wall parts. Axial and shear forces are transferred from concrete to steel plate or from steel plate to concrete by means of direct pressure and interface friction between the steel and the concrete, and also by the tie bars distributed along the wall surface at specified intervals.

Capacity-based design principles are followed in the design of C-PSW/CF. The wall is assumed to attain plastic moment capacity at the base: the steel plates are assumed to attain their yield strength, and the concrete is assumed to reach its unconfined compressive strength. Because of constructional appeal such as modular construction, construction speed, functionally (being used as formwork, falsework) off-site fabrication, and structural appeal such as ductility, high-stiffness and strength, C-PSW/CF have been extensively researched in the last two decades (e.g. Oduyemi and Wright (1989), Wright et al. (1991), Bowerman et al. (1999), Xie and Chapman (2006), Eom et al. (2009), Ramesh (2013), Alzeni and Bruneau (2017), Polat and Bruneau (2017, 2018), Varma et al. (2019), and Kenarangi et al. (2021)).

Polat and Bruneau (2018) showed that axial forces on the steel plate were redistributed to infill concrete following the steel plate local buckling. Polat et al. (2021) and Polat (2022) showed that tie bars axial force demands in planar C-PSW/CF result from the prying action of the steel plate and the confinement action of the infill concrete. The prying action is introduced by steel plate local buckling following yielding under wall flexural deformation and is related to prying length and through-thickness plastic moment of the steel plate. The concrete confinement action is introduced under wall flexure and large compressive strains developed within the concrete. Arching action is assumed to form within the concrete under compression between the adjacent tie bars in the vertical axis. Theoretical models were developed

* *Corresponding author*. Tel.: +90-428-213-1794 ; E-mail address: erkanpolat@munzur.edu.tr (E. Polat)
ISSN: 2149-8024 / DOI: https://doi.org/10.20528/cjsmec.2022.04.005

to predict the tie bars axial force demands due to prying action (Polat et al. 2021) and to predict the tie bars axial force demands due to confining action (Polat 2022). However, although the walls examined in these studies did not have boundary plates, in practice, boundary plates can often be preferred because they both increase the strength of the wall and form a formwork for concrete placement. This study aims to investigate the influence of round and planar boundary plates, which are frequently used for C-PSW/CF, on the axial force demands of the tie bars. In addition, this study shows that the theoretical models developed by Polat (2022) based on walls without boundary plates to predict tie bar maximum force demands are conservative and can also be applied for walls with boundary plates.

2. Wall Geometry and Properties

Fig. 1(a-c) illustrates the cross-sections of the wall models. Note that the wall model shown in (c) was designed and tested by Alzeni and Bruneau (2017) and was used as a reference for the other wall geometries shown in (a) and (b). Wall cross-sections consist of steel web plates, infill concrete and boundary plates. The location of the tie bars, extending between the dual steel web plates, are also indicated in the Figure. Model NB, shown in the Fig. 1(a), has no boundary plates. Models B1 and B2, shown in Fig. 1(b-c), have boundary elements in the form of planar and round plates, respectively. Except for the boundary plates, the walls have otherwise the same geometry and dimensions.

Fig. 2 shows a representative wall dimension in elevation and plan view for Model NB. All Models has a height of 3048mm, infill concrete thickness of 203.2mm, steel web plate and boundary plate thickness (t_s) of 7.94mm, tie bar diameter of 25.4mm. The total depths of the cross-sections are 1016mm, 1025.5mm and 1235mm for Models NB, B1 and B2; respectively. The tie bars are spaced 203.2 mm horizontally (w_2) and vertically (w_1), except that the horizontal distance between the last two rows is 152.4 mm. The slenderness of the steel web plate given by the ratio of vertical tie spacing to plate thickness (w_1/t_s) equal to 25.6 for all Models. The reinforcement ratio (calculated as the ratio of steel area to concrete area) is 7.8%, %9.4, and %8.96 for Models NB, B1 and B2, respectively. Accordingly, all Models have satisfactory reinforcement ratio with regards to AISC 341-22 Seismic Provisions (AISC 2022) where the reinforcement ratio for C-PSW/CF is limited to 1-10%.

The infill concrete has uniaxial compressive strength of 47.8 MPa. The steel web and boundary plates have a yield strength of 427 MPa, an elastic modulus of 205463 MPa. For the tie bars, elastic material properties were used. Note that six tie bars were identified in Fig. 1(a) and denoted as; Tie_{11}, Tie_{12} for the first row Tie_{21}, Tie_{22} for the second row, and Tie_{31}, Tie_{32} for the third row. In Section 4, the axial force demand on these tie bars will be used to compare for Models NB, B1 and B2 under monotonic lateral displacement.

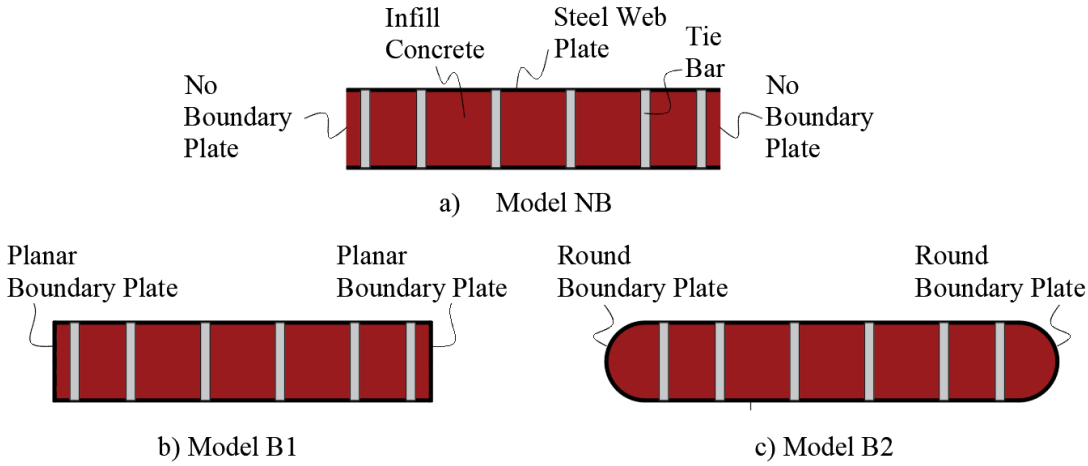

Fig. 1. Illustration of wall cross-sections: (a) Model NB; (b) Model B1; and (c) Model B2.

3. Finite Element Modeling

3.1. Element and material models

Finite element (FE) models of the walls were developed using LS-Dyna (LSTC 2022). Fig. 3 shows the isometric views of the developed FE models. Since the walls were symmetrical with respect to the loading direction, the walls were modeled only in half using the symmetry boundary conditions. In terms of elements, four node fully integrated shell element was used for modeling the web and boundary plates, eight node constant stress solid element was used to model the concrete and two node beam element was used to model the tie bars. In terms of element sizes, each solid element was 25.4x25.4x25.4mm, each shell element was 25.4x25.5, and each beam element was 25.4mm. For modeling the tie bars, the slip model developed by Polat et al. (2021) was used. In this model, tie bars extending between the steel plates are restrained to infill concrete in the two orthogonal transverse directions (i.e., X and Z axes) and unrestrained in its own axis (i.e., Y axis); allowing development of uniform axial force along the tie bars. For typical half-symmetric FE model, for example for Model NB, a total of 19200 solid elements, 4800 shell elements, and 360 beam elements were used.

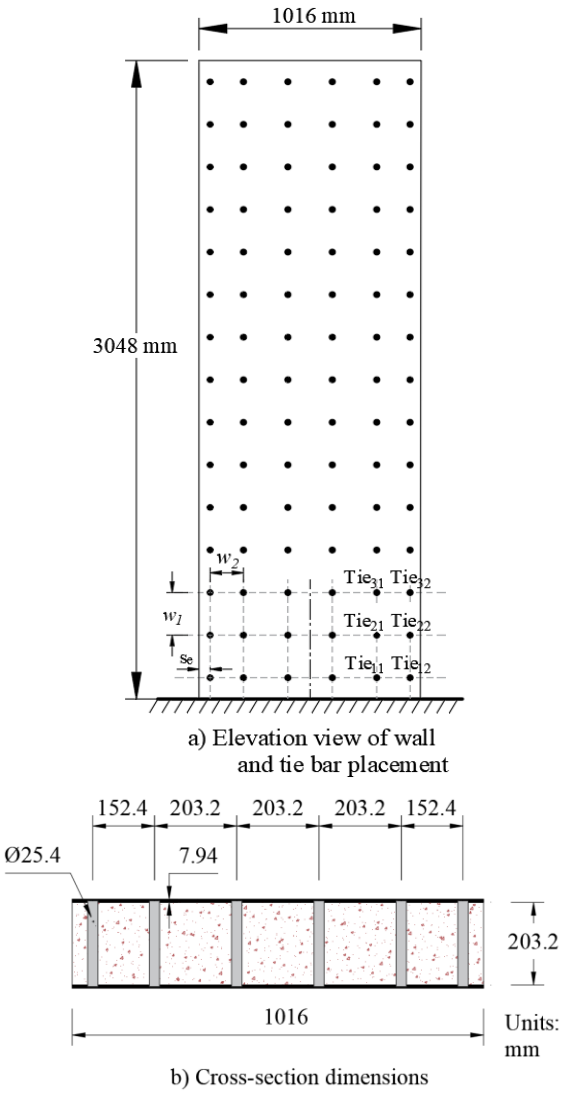

Fig. 2. Dimensions of Model NB in: (a) Elevation view of wall and tie bar placement; and (b) Cross-section.

For modeling the concrete, the Karagozian & Case Concrete Model – Release III (KCC) was used. The selection of this model is based on prior studies (Polat 2020; Polat et al. 2021) that have shown that walls with KCC can reasonably predict the ultimate strength of the walls tested while simulating concrete dilation. For modeling the steel, the plastic-kinematic material model was used. This model is represented by bi-linear curves with elastic and post-elastic modulus. The same material model with elastic properties was used for modeling the tie bars. Note that, Model B2 was developed previously with base footing (with different concrete material model and without tie bar slip model) by Polat and Bruneau (2017) and benchmarked against tested specimen (Alzeni and Bruneau 2014; Alzeni and Bruneau 2017). Model NB is the same model considered in the investigation of tie bars axial force demands in C-PSW/CF without boundary plates by Polat et al. (2021).

3.2. Finite element analysis

The Models were subjected to static displacement at the top. Implicit solution procedure of the program was used for the inelastic nonlinear analysis of the Models. The maximum time step for the nonlinear analysis was set to 0.01second (resulting in hundred steps for a total of 1 second loading curve). Using 4-core dedicated processors, a typical analysis duration was about two hours. Fig. 4(a-c) shows the pushover curves of the walls under monotonic lateral displacement. The maximum lateral load carrying capacity was 917 kN for Model NB, 1265 kN for Model B1, and 1660 kN for Model B2. Model NB exhibited gradual strength degradation as a result of steel plate local buckling and lack of boundary element. For example, it has a wall strength of 860 kN at 4% drift, corresponding to a strength loss of about 7%. Strength degradation for Models B1 and B2 was limited, attributed to having boundary plates in these Models.

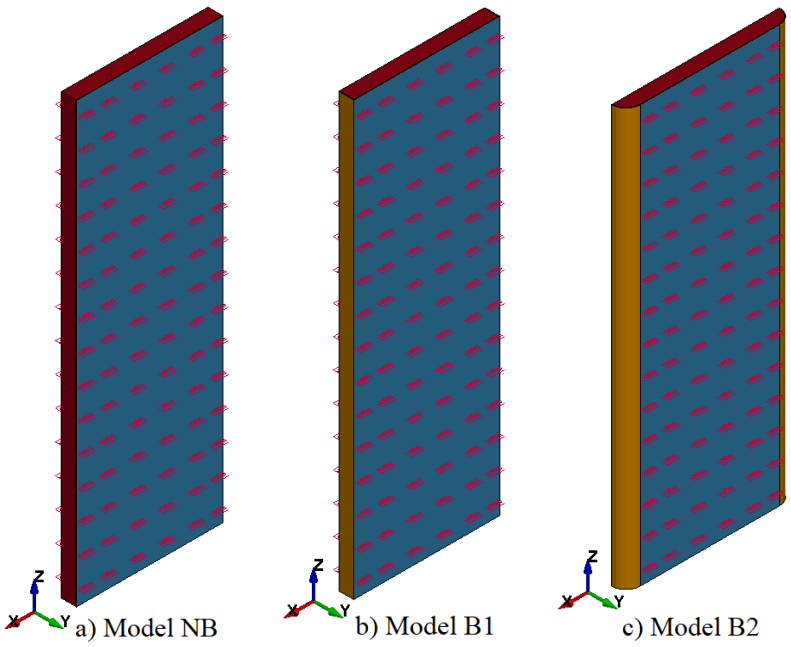

Fig. 3. Isometric views of the half-symmetric FE models of: (a) Model NB; (b) Model B1; and (c) Model B2.

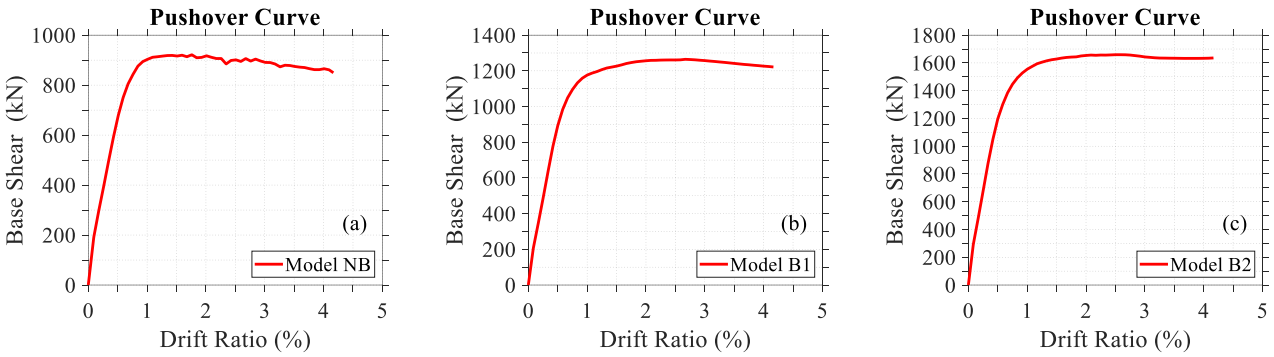

Fig. 4. Pushover curves of: (a) Model NB; (b) Model B1; and (c) Model B2.

3.3. Passive lateral pressure on boundary plates

Fig. 5(a-c) shows the contours of interface normal forces forming under flexural wall deformation for Models NB, B1 and B2. It should be noted that interface normal forces are nodal forces formed at the steel plate-concrete interface. Under wall flexure, the part of the concrete under compression expands laterally due to Poisson affect and shear dilation. The lateral expansion of concrete is restrained by the steel plates and tie bars which provides passive lateral pressure on concrete surface. Interfacial pressures can be obtained by first obtaining the interfacial normal forces at the interface nodes of steel plates then dividing these forces by the effective area. Therefore, the contours shown in the Figure can be interpreted as pressure contours other than the numerical values shown.

The highest values for passive lateral pressures occur in the region where the lateral expansion of the concrete is restrained by the tie bars and boundary plates. Tie bars provides lateral restraint by means of axial stiffness whereas boundary plates provide lateral restraints by means of transverse plate stiffness. Because Model NB has no boundary plate, tie bars located at the very bottom of the wall on the compression side were subjected to larger axial force demands. However, for Models B1 and B2, boundary plates contributed to transverse force resistance of the tie bars against concrete lateral expansion, so the tie bars of these Models received less axial force demands. Because of the round shape of the boundary plate of Model B2, the passive lateral pressures (or interface normal forces) were more evenly distributed, while lateral pressures were concentrated at the corner of the planar boundary plate of Model B1.

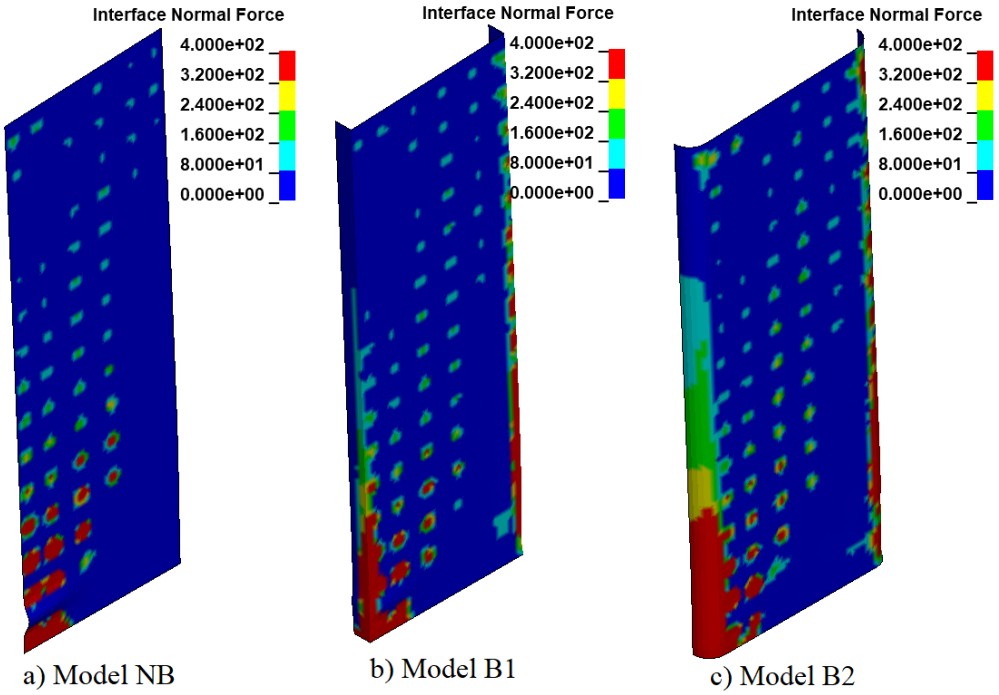

Fig. 5. Interface pressure acting on steel plate of: (a) Model NB; (b) Model B1; and (c) Model B2.

Although Fig. 5 provides useful information about the formation of passive lateral pressures, it cannot be interpreted reasonably for an understanding of the actual magnitude of the pressure distribution. To facilitate the interpretation of the actual magnitude of pressure distribution, three-dimensional pressure distribution over a selected partial region of the boundary plates were plotted.

Fig. 6(a-b) shows these selected partial regions in Models B1 and B2 boundary plates. Fig. 7(a-b) shows the three-dimensional interface pressure distributions on the boundary plates of Models B1 and B2. Note that, interface pressures were obtained by dividing the interface force created at each node of the shell element by the corresponding tributary surface area of the element. As shown in Fig. 7(a), interface pressures reach their maximum where the planar boundary plate meets the web plate. The interface pressures decrease almost linearly from the maximum points and drop to zero at quarter wall thickness from the edge. As shown in Fig. 7(b), interface pressures are more evenly distributed over the interface area of the round boundary plate. Note that, slightly above the wall base, pressures drop in these areas as a result of plate local buckling in the round boundary plate. Compared to the pressure distribution on the planar plate, the pressure distribution on the round plate is more uniform and is distributed higher elevation.

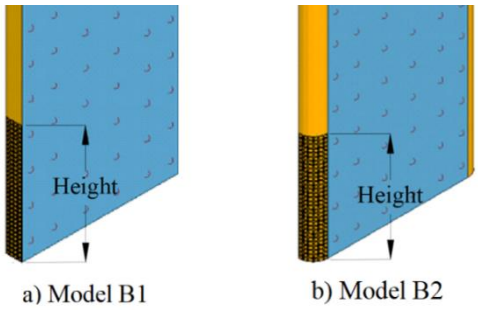

Fig. 6. Selected location of boundary plates of: (a) Model B1; and (b) Model B2 for 3D interface pressure distribution.

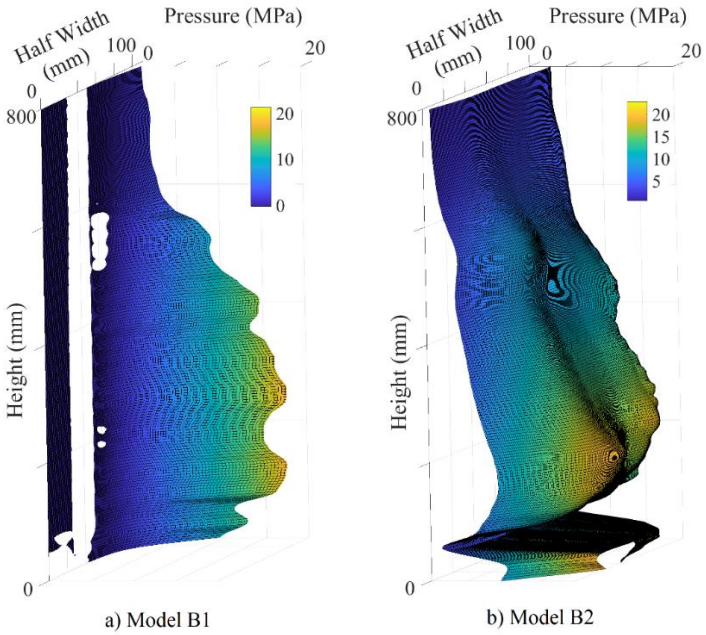

Fig. 7. 3D interface pressure distribution on boundary plates of: (a) Model B1; and (b) Model B2.

4. Comparison of Tie Bar Axial Forces

Fig. 8(a-f) compares axial force demands of the six tie bars (Tie_{11}, Tie_{12}, Tie_{21}, Tie_{22}, Tie_{31}, Tie_{32}) identified previously. For all Models, the tie bars closest to the wall boundary received larger axial force demands than the interior tie bars. This behavior is explained by the increase in concrete dilation as a result of increased axial strain demand on the concrete. Tie bars axial force demands decreased with distance from the wall base. Exception to this was observed in the second row of tie bars (i.e., Tie_{21}, Tie_{22}). For these bars, plate local buckling contributed to axial force demands (note that steel plate local buckling take place between the first and second row of tie bars). It should be noted that tie bars receive additional axial force demand due to prying action in addition to the confining action (Polat et al. 2021; Polat 2022). All the tie bars in Model NB received greater axial force demands than tie bars in Models B1 and B2. All the tie bars in Models B1 and B2, except the first-row tie bars (i.e., Tie_{11}, Tie_{12}), received similar axial force demands. But for the first-row tie bars, the axial force demands in Model B1 are greater than in Model B2. This is attributed to the fact that the round boundary plate contribution to concrete confinement better than the planar plate. To demonstrate this, Fig. 9(a-b) shows the force variation in the transverse direction on the boundary plates along the wall height for Models B1 and B2. The transverse forces were obtained by multiplying the transverse stresses on the shell element with the area of the shell element in the transverse direction. Force demands were obtained at 0.5%, 1.0%, 2.0%, 3.0% and 4.0% wall drift ratios. For both Models, the transverse force demands on the boundary plates increase with increasing wall drift. For Model B2, the curves are smoother while for Model B1 they are slightly jagged. While transverse forces on the planar boundary plate were almost limited to a height of plastic hinge (1000mm) for Model B1,

transverse forces on the round boundary plate of Model B2 were spread out almost to the height of the wall. This is important in terms of showing the effectiveness of the round boundary plate compared to the planar one. Comparison of tie bars axial force demands for walls with and without boundary plates in Fig. 8(a-f) demonstrate that the theoretical models developed by Polat (2022) based on walls without boundary plates to predict tie bar maximum force demands are conservative and can also be applied for walls with boundary plates.

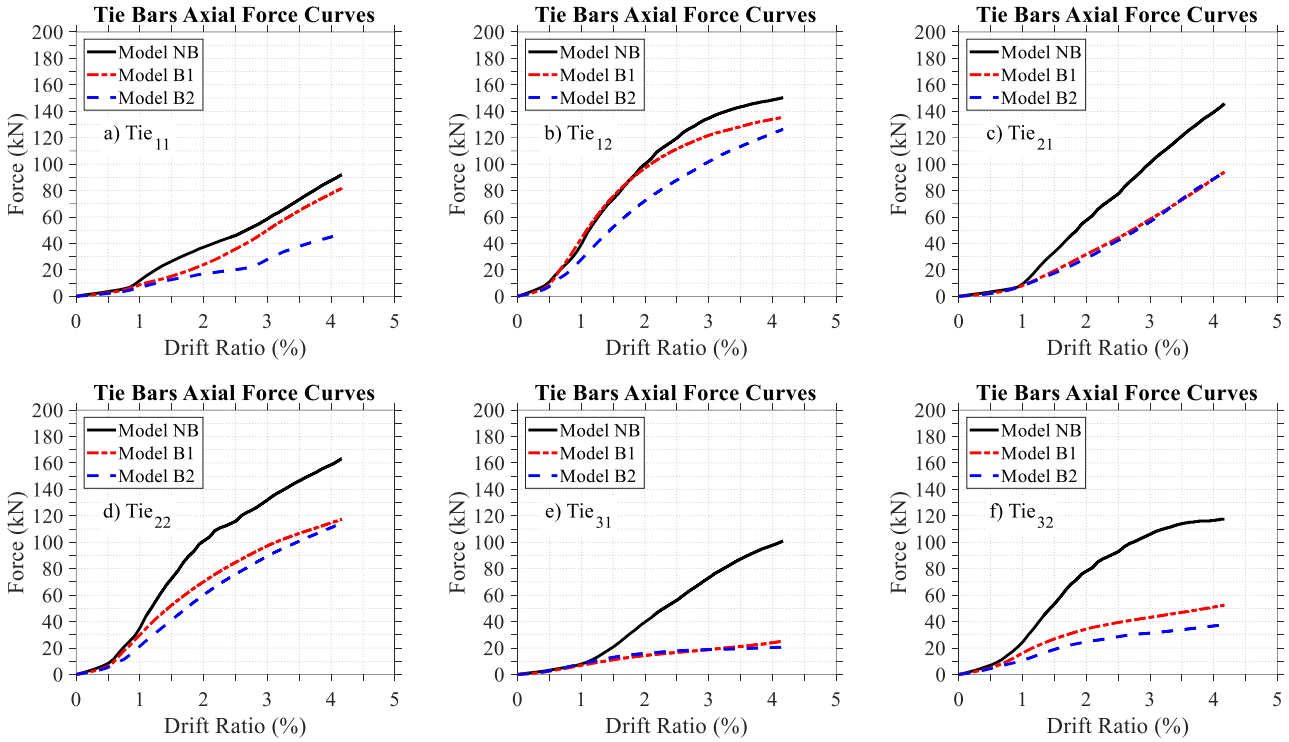

Fig. 8. Comparison of bar axial force demand in Models NB, B1 and B2 for: (a) Tie11; (b) Tie12; (c) Tie21; (d) Tie22; (e) Tie31; and (f) Tie32.

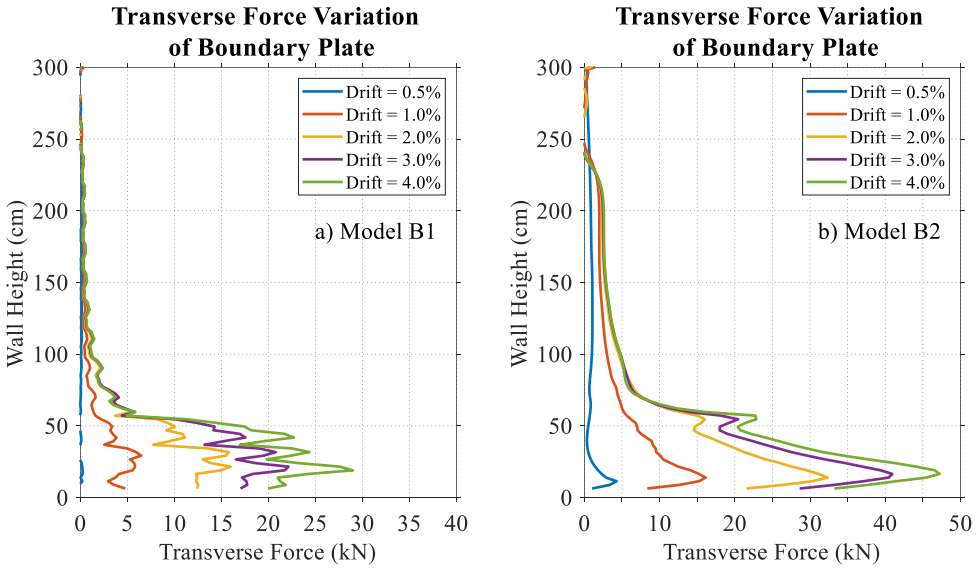

Fig. 9. Transverse force variation along the height of wall boundary elements: (a) Model B1; and (b) Model B2.

5. Conclusions

The influence of boundary plates on tie bar axial force demands in planar C-PSW/CF was numerically investigated. Three-dimensional finite element wall models were developed. Three planar C-PSW/CF were used, two of which had boundary elements consisting of planar and round plates. The models were subjected to monotonic displacement up to 4% drift ratio. The findings from the numerical results are as follows:

- Inclusion of boundary plates resulted in a decrease in tie bars axial force demands. This applies to both types of boundary plates.
- Except for the tie bars located at the very bottom of the wall, the tie bars received almost similar axial force demands for both type of boundary plates.
- Compared to the wall without boundary plate, tie bar axial force demands in the walls with boundary plates decreased significantly with distance from the base of the wall.
- The theoretical models developed previously by Polat (2022) based on walls without boundary plates to predict tie bar maximum force demands are conservative and can also be applied for walls with boundary plates.
- Passive lateral pressures are more evenly distributed on the round plate but spread towards the corners on the planar plate. This is important for the connection between the boundary plates and the web plates. Pressure concentration on the plate corners may require more rigorous connection design between the boundary plates and web plates.
- The round boundary plate takes greater transverse force demands than the planar plate, especially contributing more to the confining force resistance of the first-row tie bars, thus helping to decrease force demands on these tie bars.

Acknowledgements

None declared.

Funding

The author received no financial support for the research, authorship, and/or publication of this manuscript.

Conflict of Interest

The author declared no potential conflicts of interest with respect to the research, authorship, and/or publication of this manuscript.

References

AISC (2022). Seismic provisions for structural steel buildings. AISC 341-22, American Institute of Steel Construction, Chicago, IL.

Alzeni Y, Bruneau M (2014). Cyclic inelastic behavior of concrete filled sandwich panel walls subjected to in plane flexure. *Technical Rep. MCEER, 14-009*, Univ. at Buffalo, the State Univ. of New York, Buffalo, NY, MCEER.

Alzeni Y, Bruneau M (2017). In-plane cyclic testing of concrete-filled sandwich steel panel walls with and without boundary elements. *Journal of Structural Engineering*, 143(9), 04017115.

Bowerman H, Gough M, King C (1999). Bi-Steel Design and Construction Guide. British Steel Ltd, Scunthorpe, London.

Eom T-S, Park H-G, Lee C-H, Kim J-H, Chang I-H (2009). Behavior of double skin composite wall subjected to in-plane cyclic loading. *Journal of Structural Engineering*, 135(10), 1239-1249.

Kenarangi H, Kizilarslan E, Bruneau M (2021). Cyclic behavior of c-shaped composite plate shear walls–Concrete filled. *Engineering Structures*, 226, 111306.

LSTC (2022). Livermore Software Technology Corporation, version R8.0.Livermore Software Technology Corporation, Livermore, CA.

Oduyemi T, Wright H (1989). An experimental investigation into the behaviour of double-skin sandwich beams. *Journal of Constructional Steel Research*, 14(3), 197-220.

Polat E (2020). Investigation of influence of concrete material models on cyclic inelastic response of a concrete filled composite plate shear wall. *Challenge Journal of Structural Mechanics*, 6(2), 91-98.

Polat E (2022). Theoretical models for tie bar maximum axial force demand in composite plate shear walls–concrete filled. *International Journal of Steel Structures*, 22(4), 1108-1125.

Polat E, Bruneau M (2017). Modeling cyclic inelastic in-plane flexural behavior of concrete filled sandwich steel panel walls. *Engineering Structures*, 148, 63-80.

Polat E, Bruneau M (2018). Cyclic inelastic in-plane flexural behavior of concrete filled sandwich steel panel walls with different cross-section properties. *Engineering Journal, American Institute of Steel Construction*, 55, 45-76.

Polat E, Kenarangi H, Bruneau M (2021). Investigation of tie bars axial force demands in composite plate shear walls—concrete filled. *International Journal of Steel Structures*, 21(3), 901-921.

Ramesh S (2013). Behavior and design of earthquake-resistant dual-plate composite shear wall systems. Technical Report, Purdue University.

Varma AH, Shafaei S, Klemencic R (2019). Steel modules of composite plate shear walls: Behavior, stability, and design. *Thin-Walled Structures*, 145, 106384.

Wright H, Oduyemi T, Evans H (1991). The experimental behaviour of double skin composite elements. *Journal of Constructional Steel Research*, 19(2), 97-110.

Xie M, Chapman J (2006). Developments in sandwich construction. *Journal of Constructional Steel Research*, 62(11), 1123-1133.